

Astrometry Survey Missions Beyond the Magnitude Limit

Samir Salim, Andrew Gould

Ohio State University, Department of Astronomy, 140 W. 18th Ave., Columbus, OH 43210

samir@astronomy.ohio-state.edu

gould@astronomy.ohio-state.edu

and

Rob P. Olling¹

Department of the Navy, USNO, 3450 Massachusetts Ave NW, Washington, DC 20392-5420

olling@usno.navy.mil

ABSTRACT

Three planned astrometry survey satellites, *FAME*, *DIVA*, and *GAIA*, all aim at observing magnitude-limited samples. We argue that substantial additional scientific opportunities are within the reach of these mission if they devote a modest fraction of their catalogs to selected targets that are fainter than their magnitude limits. We show that the addition of $\mathcal{O}(10^6)$ faint ($R > 15$) targets to the 40×10^6 object *FAME* catalog can improve the precision of the reference frame by a factor 2.5, to $7 \mu\text{as yr}^{-1}$, increase Galactocentric distance at which halo rotation can be precisely (2 km s^{-1}) measured by a factor 4, to 25 kpc, and increase the number of late M dwarfs, L dwarfs, and white dwarfs with good parallaxes by an order of magnitude. In most cases, the candidate quasars, horizontal branch stars, and dim dwarfs that should be observed to achieve these aims are not yet known. We present various methods to identify candidates from these classes, and assess the efficiencies of these methods. The analysis presented here can be applied to *DIVA* with modest modifications. Application to *GAIA* should be deferred until the characteristics of potential targets are better constrained.

Subject headings: astrometry—Galaxy: fundamental parameters—Galaxy: halo—reference systems—stars: late-type—white dwarfs

¹Universities Space Research Association, 300 D Street, SW, suite 801, Washington, DC 20024-4703

1. Introduction

The baseline designs of the three planned astrometry satellites *FAME*, *DIVA*, and *GAIA*, call for magnitude-limited samples. By contrast, *Hipparcos* defined only about half of its sample by a magnitude limit (which ranged from $V < 7.3$ to $V < 9$), while the remaining stars were chosen based on a variety of specific scientific programs and objectives. Does the magnitude-limited approach represent a logical choice for future astrometry missions, or does a large fraction of their potentially achievable science lie beyond the magnitude limit, as it did for *Hipparcos*?

Certainly there are strong arguments for choosing most of the new-satellite samples by magnitude. For one, these surveys will be so large, $\sim 10^{7.6}$ stars for *FAME* and *DIVA* and $\sim 10^9$ for *GAIA*, that almost nothing is known about this many stars other than their magnitudes and (to some extent) their colors. By contrast, *Hipparcos* had access to catalogs of high proper-motion, nearby, and other classes of special stars whose sizes were a substantial fraction of its much smaller $\sim 10^5$ star catalog. Also, the astrometric precision of the new missions falls off rapidly with flux, either $\sigma \propto \text{flux}^{-1/2}$ in the photon-noise regime or $\sigma \propto \text{flux}^{-1}$ in the read-noise regime. Thus it seems logical to focus the effort on the stars for which the astrometry is best. This effect was much less compelling in the case of *Hipparcos* for which the astrometric precision fell off only by a factor ~ 2 between $V = 7.3$ and $V = 11.5$ (because it was able to devote longer exposures to fainter objects). Finally, if *Hipparcos* had established its full catalog simply by setting a magnitude limit (at about $V \sim 9$), whole classes of stars would have been virtually absent, including M dwarfs, white dwarfs, and radio stars that link the optical and radio frames. The new missions will go so much deeper that they will contain substantial samples of all of these various objects, even without any special effort.

Although these arguments have some merit, we believe that if the new missions maintain their purely magnitude-limited approach, they will miss out on major scientific opportunities. Some of these losses are obvious. For example, dim stars (like white dwarfs and M dwarfs) are relatively quite close even when they lie below the magnitude limit, and hence they can have relative parallax errors that are very small even though their absolute astrometry is poor. But as we will show, there are other, less obvious faint objects that can have huge scientific returns despite the fact that they are so far away that their *parallaxes* cannot be even crudely measured. Moreover, once one recognizes the importance of observing these various categories of faint objects, it is far from obvious how to assemble the samples, which are likely to contain $\mathcal{O}(10^6)$ stars, most of which are not known to be in the designated classes, or are not yet identified.

Here we examine what general classes of faint stars should be considered as potential

observing targets by astrometric missions, despite the fact that in some cases, each faint star so chosen may displace some bright star which would have yielded better astrometry. We review how *Hipparcos* handled these classes and then look forward to future missions. We identify a few major science questions that can be attacked if *FAME* or *DIVA* chooses to observe faint stars. We make quantitative estimates of how well *FAME* will be able to address these questions with and without the observation of faint stars and assess various approaches to constructing an input catalog which *FAME* requires. The principles that we outline can be applied directly to *DIVA*, so we do not repeat the analysis for it. We briefly discuss how these principles will apply to *GAIA*, but argue that a detailed analysis is not warranted until closer to mission launch.

We do not believe that we have exhausted the scope of interesting faint stars that could be added to future mission catalogs. Our goal is rather to present a few classes of additional stars that could have major scientific impact and to illustrate both the promise and the difficulties of including them. We hope that this will encourage others to explore the potential of other categories of stars and to improve on the methods that we outline here for selecting the candidates.

In the next subsection we analyze target selection for *Hipparcos* catalog in terms of magnitude-limited vs. faint sample. In § 1.3 we introduce the methodology of non-magnitude selected samples to future astrometric missions. These missions are described in general in § 1.2, while their astrometric performance is evaluated in § 2. In §§ 3-6 we apply this methodology to *FAME*, as a specific example². In § 7 we discuss how this methodology can be applied to *GAIA* and *DIVA*.

1.1. The *Hipparcos* Experience

The magnitude-limited component of the *Hipparcos* catalog comprises roughly 50,000 stars that satisfy $V < 7.3 + 1.1 \sin |b| + \Delta V$, where $\Delta V = 0.6$ for spectral types G5 and earlier and is zero otherwise. The remaining roughly 70,000 stars (with $7.3 < V \lesssim 11.5$) were chosen from among 214,000 submitted to ESA in 214 separate proposals. Neither the proposals themselves, which supported science projects ranging from the sub-dwarf distance scale to improvement of the lunar orbit, nor the process of selection can be properly reviewed

²After submitting the manuscript, the *FAME* mission, at least in the form we present it here, has been cancelled by NASA. Efforts are presently being made to continue the project. In any case the methodology, the proposed scientific objectives, and the target selection methods are applicable to astrometry missions in general.

here. The most important points we want to make can be understood by inspection of Figure 1, which shows the proper-motion distributions of *Hipparcos* stars that lie respectively within or beyond the magnitude limit. The first point to note is that the great majority ($\sim 70\%$) of the stars with proper motions exceeding the $\mu = 180 \text{ mas yr}^{-1}$ limit of the Luyten (1979, 1980) NLTT catalog are drawn from beyond the magnitude limit. This is because *Hipparcos* included essentially all NLTT stars that lie within its range ($V \lesssim 11.5$). Over 99% of the roughly 1000 intrinsically dim ($M_V > 8.5$) stars in the *Hipparcos* catalog lie beyond its magnitude limit, and of these almost 90% come from the NLTT. Thus, while various additional sources of dim stars were exploited (like nearby stars), proper-motion selection was the most effective method for including them.

The second point to note, however, is that the great majority of the added stars have very low proper motions, $\mu \sim 15 \text{ mas yr}^{-1}$, meaning that they probably lie at distances of order 500 pc, which implies that their parallaxes could hardly be measured by *Hipparcos*. The science drivers for these stars are varied, but in most cases knowledge of their distances was not critical. For example, for stars that were to be occulted by the Moon, only the positions and proper motions would be of interest. Similarly, RR Lyrae star proper motions would be useful for a statistical parallax measurement even though their trig parallaxes were marginal at best. Another 200 stars were chosen because they lay close to quasars, the hope being to eventually use these to tie together the *Hipparcos* and extragalactic reference frames. Again, no parallaxes are needed to make this tie-in.

Thus, the main lesson from *Hipparcos* is that there can be a wide variety of reasons for extending the catalog beyond the magnitude limit. In some cases, this may be the only way to obtain good parallaxes of special classes of stars, but in other cases the parallaxes may be of no interest.

1.2. Future Missions

Four major astrometry missions are planned for the next decade, *FAME*, *DIVA*, *GAIA* and *SIM*. Three of these exploit the same basic principle of the scanning telescope, employed first by *Hipparcos*. *FAME*³ (USNO 1999) is a NASA mission proposed by United States Naval Observatory (USNO). *FAME*'s design specifications promise twenty-fold improvement in astrometric precision over *Hipparcos* in the $5 < R < 10$ range, down to 0.5 mas precision at the survey limit of $R = 15$. Its aim is to obtain astrometry, as well as photometry in two Sloan bands (r' and i'), of $\sim 4 \times 10^7$ stars, over a 5 yr planned mission duration.

³*Full-Sky Astrometric Explorer*: <http://www.usno.navy.mil/FAME/>

The German-built satellite *DIVA*⁴ is now near final approval. It is expected to observe a similar number of stars, but only for 2 years and with somewhat smaller mirrors. Hence it should achieve several times less precise astrometry than *FAME*. In addition, *DIVA* expects to obtain 30-element spectral photometry. Both *FAME* and *DIVA* aim to launch in 2004.

The much more ambitious *GAIA*⁵ mission will obtain an order of magnitude better performance than *FAME*. It will observe $\mathcal{O}(10^9)$ objects to $V = 20$ including not only astrometry, but photometry and radial velocities as well. However, *GAIA*'s earliest launch date is 2011. Also planned for this epoch is the *Space Interferometry Mission (SIM)*, which will be yet more precise. However, since *SIM* is a targeted rather than a survey mission, it does not fall within the framework of the present study.

1.3. Scope and Method

Following the experience of *Hipparcos*, there are two broad categories of potential additional targets that lie beyond the magnitude limit: those that are so dim (and hence so close) that one could obtain useful parallaxes even with relatively poor astrometry, and those for which the positions and proper motions are of interest even when the parallaxes may be unmeasurable. While these lessons are very general, their application is not. When the flux limit falls by a factor 100 or 1000, as it does when going from *Hipparcos* to *FAME* or from *FAME* to *GAIA*, the very classes of objects that fit into these two broad categories can change completely. The problems in identifying members of these classes change completely as well. For example, *Hipparcos* observed 10,000 stars that are occulted by the Moon, the majority of which were beyond the magnitude limit. *FAME*, by contrast, will observe about 3 million such stars *within* its magnitude limit, far more than could be used in any conceivable lunar-orbit or lunar-topography investigation. On the other hand, consider quasars, a class of objects whose proper motions are of interest because they are known a priori to be zero. *Hipparcos* observed precisely one of these (3C 273), and the proper-motion error of this measurement, $\sigma_\mu \sim 6 \text{ mas yr}^{-1}$, turned out to be so large as to render it useless. The *Hipparcos* reference frame was in fact fixed to radio stars, not directly to quasars. By contrast, as we discuss in detail in § 3.2, the *FAME* reference frame can be fixed with exquisite precision by observing $\mathcal{O}(10^5)$ quasars, the vast majority of which lie beyond the magnitude limit, and indeed are yet to be discovered.

⁴<http://www.ari.uni-heidelberg.de/diva/>

⁵ <http://astro.estec.esa.nl/GAIA/>

Thus, our approach will be to apply the very general lessons from *Hipparcos* to the concrete situation of *FAME*. We will address both the questions of what science can be obtained by going beyond the magnitude limit, and of how one can find the often unclassified targets. The characteristics of the *DIVA* mission are similar enough to those of *FAME* that the range of possible science projects will be similar. As we discuss in § 7, the science achievable beyond *GAIA*’s magnitude limit can only be sketched at the present time.

2. Astrometric Performance of Survey Missions

Generically, one expects three regimes of precision for an astrometric satellite: systematics limited, photon limited, and read-noise limited, for bright, middle, and faint stars respectively. Here, our focus is on the latter two regimes, where the astrometric errors should scale as $\sigma \propto \text{flux}^{-1/2}$ and $\sigma \propto \text{flux}^{-1}$, respectively. The one-dimensional positional accuracy of an object after a mission of duration t is then given by an expression of the form,

$$\sigma = \sigma_0 \sqrt{\frac{5 \text{ yr}}{t}} 10^{0.2(m-15)} [1 + c_{\text{RN}} 10^{0.4(m-15)}]^{1/2}, \quad (1)$$

where m is the astrometric-band magnitude, and where we have scaled the mission duration to 5 yr, and the magnitude to $m = 15$. Equation (1) contains two constants that need to be determined: the normalization factor σ_0 , and the read-out noise coefficient c_{RN} . In fact, since all future missions are planning to use an *Hipparcos*-like scanning law, which has highly uneven coverage, the “constant” σ_0 is actually a function of ecliptic latitude. For statistical studies of the type investigated here, it is appropriate to take an average value.

Proper-motion accuracies for equally spaced observations are related to positional accuracies by

$$\sigma_\mu = \sqrt{12} \frac{\sigma}{t} \quad (2)$$

While *Hipparcos*-like observations are not precisely equally spaced, this formula remains accurate for mission lifetimes of at least 2 yr.

Parallax accuracies depend on the ecliptic latitude of the object, and range from $\sigma_\pi = \sigma$ at the ecliptic poles to $\sigma_\pi = \sqrt{2}\sigma$ on the ecliptic, again assuming uniform sampling. Since there will be some times of the year when no observations are carried out, the actual parallax precision will not be given as simply, and will be somewhat worse. For *FAME*, Murison (2001) uses a realistic scanning law and finds that on average,

$$\sigma_\pi \simeq 1.43\sigma, \quad (3)$$

(see also Olling 2001), which we will use here. This coefficient should depend only very weakly on the precise mission characteristics.

2.1. Specific Estimates

For the three proposed missions, the parameters entering equations (1)–(3) are approximately given by

$$\sigma_0 = 240 \mu\text{as}, \quad c_{\text{RN}} = 1.06, \quad m = R, \quad t = 5 \text{ yr.} \quad (\text{FAME}) \quad (4)$$

$$\sigma_0 = 965 \mu\text{as}, \quad c_{\text{RN}} = 1.91, \quad m = R, \quad t = 2 \text{ yr.} \quad (\text{DIVA}) \quad (5)$$

$$\sigma_0 = 1.8 \mu\text{as}, \quad c_{\text{RN}} = 0.012, \quad m = V, \quad t = 5 \text{ yr.} \quad (\text{GAIA}) \quad (6)$$

Since in all cases the actual astrometric bands differ from the standard bands in these equations, the parameters vary slightly with stellar type. For example, for *FAME* $|R - m|$ is typically small, but does rise to $R - m = 0.27$ for an M7 dwarf. Throughout this paper we refer to R magnitudes (and not V , for example) to describe *FAME* sensitivity. In our actual calculations we take account of the small differences between the *FAME* astrometric band and R as a function of spectral type, although in practice this makes very little difference. Corrections to convert V to m for stars of different temperatures are given in Olling (2001).

From equations (4)–(6), the three missions reach the read-noise limit (where photon noise equals read noise) at $R = 15.0$, $R = 14.3$, and $V = 19.8$. These are also approximately the magnitude limits of these surveys ($R \sim 15$, $R \sim 15$, and $V \sim 20$). Nevertheless, while the astrometric precision obviously deteriorates rapidly beyond these limits, the scientific potential from observing carefully chosen fainter objects is high. In the following three sections we illustrate this point, specifically using the *FAME* parameters (eq. [4]). In § 7, we briefly discuss *DIVA* and *GAIA*.

3. Quasar Reference Frame

In order to be able to translate relative proper motions to absolute ones, the reference frame must be “anchored” to a quasi-inertial frame: the satellite must observe a number of objects that have essentially no proper motion, and whose light profile is stellar, or objects that move but whose absolute proper motion is known with great precision. With the roughly 100 quasars that fall within *FAME*’s survey limits, the frame can be fixed only with a precision of $\approx 19 \mu\text{as yr}^{-1}$ (in one direction).

Further refinement of the rotation of the *FAME* frame is possible by including in the input catalog quasars (or quasar candidates) with $R > 15$. The precise fixing of the reference frame is important as it allows the motion of certain populations of stars to be determined with much greater accuracy, especially increasing the fractional accuracy for slow-moving populations. Such measurements will be described in more detail in the §§4.1. and 4.4. Of perhaps even greater general importance, measuring the ‘parallaxes’ of objects that actually have no measurable parallaxes, such as quasars, offers a unique check on any unmodeled or unknown systematics that might affect the spacecraft while taking data, or anywhere later in the data reduction process.

The precision of the frame fixing depends on the number, distribution on the sky, and apparent brightness of the quasars that *FAME* will observe. Let $\hat{\mathbf{n}}_k = (\hat{n}_1, \hat{n}_2, \hat{n}_3)_k$, the unit vector toward the k -th quasar, be given in the rectangular Galactic coordinates, with the third component (z) perpendicular to the Galactic plane. We then form rank-3 matrix \mathbf{b}

$$b_{ij} = \sum_{k=1}^n \left(\frac{\delta_{ij} - \hat{n}_i \hat{n}_j}{\sigma_\mu^2} \right)_k ; \quad i, j = 1, 2, 3 \quad (7)$$

where σ_μ is given by equation (2) and depends on the quasar’s apparent magnitude, and δ_{ij} is the Kronecker delta. Then the reference frame accuracies along x , y , and z axes are given as square root of the diagonal terms of the covariance matrix $\mathbf{c} = \mathbf{b}^{-1}$.

3.1. Quasar (Candidate) Selection

In order to implement the frame fixing, one must specify how to build the quasar sample that *FAME* will observe and what is the number of quasars or quasar candidates in this list. The number of objects is important because we want to maximize the scientific gain (precision of the frame) without taking up too great a part of *FAME* input catalog.

Ideally, one would like to include *all* quasars in the sky down to some limiting magnitude. Obviously, with a 100% complete survey we always gain maximum astrometric signal with the least number of objects. Unfortunately the currently known sample of quasars (Veron-Cetty & Veron 2000, hereafter VV00) is complete only to $R \approx 14.5$. Completeness drops to about 50% only a magnitude fainter, and is less than 10% at $R \approx 18$. (The completeness was assessed with respect to QSO sky densities as given by Hartwick & Schade 1990. Here, and in the rest of the paper we use mean quasar colors of $B - V = 0.25$ and $V - R = 0.25$ to conveniently convert between B magnitudes used in Hartwick & Schade 1990, the mostly V magnitudes used in VV00, and our R magnitudes.)

Fortunately, there are several surveys underway that will discover new quasars over

wide areas of sky. For definiteness, we will assess what quasars are likely to be known in late 2003. We stress that the “quasar” list can actually be comprised of quasar candidates, i.e. no spectroscopic confirmation is required at the time of catalog compilation. It is only when the data are reduced at the end of the mission that spurious objects must be eliminated so that their systematic motion does not corrupt the frame. For quasar candidates that will not have their spectra taken, *FAME*’s measurements of proper motion will serve as a criterion to eliminate white dwarf contamination. For blue horizontal branch stars which are much farther away than the white dwarfs and have typical proper motion on the order of the measurement accuracy, the difference $\Delta(u' - g') \approx 1.0$ of color indices between them and quasars can be used if u' photometry is available. Otherwise, quasars can be distinguished from blue stars by their K -band excess. Quasars are also indicated by their variability which is different from that of RR Lyr stars. Eventually, the fractional contamination must be $\lesssim N_{\text{QSO}}^{-1/2}$, where N_{QSO} is the number of quasars in the sample, so that the systematic errors are smaller than the statistical ones. For any quasars candidates that lack spectroscopic confirmation and are therefore potential contaminants, one can decrease their effects on frame degradation by assigning them different weights in the fit, based on the probability of them being quasars constrained from all available (radio, optical, IR, UV, and X-ray) information.

One survey that might produce an *all-sky* sample of quasars virtually complete to beyond $R = 19$ is the *Galaxy Evolution Explorer (GALEX)*. *GALEX* is an imaging and spectroscopy space mission operating in the UV (130-300 nm) region. It will perform slitless spectroscopy of 10^5 galaxies and 10^4 quasars and obtain all-sky two-band UV photometry of 10^7 galaxies and 10^6 quasars. The two-band photometry itself will be enough to confirm the AGN-like spectral energy distribution, and thus distinguish quasars from stellar objects (mostly white dwarfs, and A-colored halo stars) (B. Peterson 2001, private communication). With the launch scheduled for January 2002, the results of the all-sky *GALEX* survey might be complete approximately at the time when the *FAME* input catalog is to be finalized (C. Martin 2001, private communication), but at the moment that remains a major uncertainty.

Hence it is prudent to determine what can be done in the absence of *GALEX* data. We expect most of the good quasar candidates to come from the Sloan Digital Sky Survey (York et al. 2000, SDSS). SDSS will also be essentially complete to beyond $R = 19$, and will perform photometry in five bands which should be very effective (70% or higher, Richards et al. 2001) in selecting the quasar candidates. More importantly, it will provide spectroscopic confirmation for almost all of the bright (by SDSS standards) candidates that are relevant for *FAME*. However, SDSS is not an all-sky survey —it covers the north polar cap ($b \lesssim 30^\circ$), and 3 strips totaling 700 deg^2 in the south polar cap, and therefore it cannot substitute for *GALEX*. Again, the issue of the status of SDSS and the availability of its data at the

time required for *FAME* is important. The current estimate (D. Weinberg 2001, private communication) is that 1/2 of the northern cap and all of the southern strips will be available.

The observing list will be further augmented by quasars found in two southern strips (750 deg^2 total) that make the 2dF Quasar Survey (Boyle et al. 2000, 2QZ), where we expect to get all quasars with $R > 16.5$. Another wide-coverage sky survey being undertaken is the FIRST Bright Quasar Survey (White et al. 2000, FBQS), in which quasars are selected by matching pointlike radio sources from FIRST to stellar-like objects with quasar colors found in Schmidt optical survey plates. The FIRST sky coverage coincides with that of SDSS so we might expect some additional candidates from the half of the northern cap that will not be available from SDSS in late 2003. The detection efficiency of FBQS is comparatively low ($\sim 25\%$), so it cannot fully substitute for the lack of SDSS coverage.

We also consider the possibility of selecting quasar candidates in regions that will not be covered by SDSS or 2QZ (50% of the northern ($b > 30^\circ$) cap and 85% of the southern ($b < -30^\circ$) cap.) To this end we investigate using the Two-Micron All-Sky Survey (2MASS) Point Source Catalog (PSC). Barkhouse & Hall (2001) have shown, using the 2nd Incremental Release of 2MASS PSC (covering $\sim 50\%$ of the whole sky), that 2MASS counterparts of the VV00 quasars occupy a distinct part in the $(B_{\text{USNO}} - J)$ vs. $(J - K_s)$ color-color diagram. The $(J - K_s)$ color of matched quasars is redder than that of stars, while $(B_{\text{USNO}} - J)$ color is moderately blue compared to the stellar range (both B_{USNO} and R_{USNO} magnitudes in 2MASS come from USNO-A2.0 catalog (Monet 1998), which is based on first generation sky survey plates). How efficient can 2MASS potentially be in detecting quasars to some apparent magnitude? In order to determine this, we simply compared the number of 2MASS-matched VV00 quasars to a complete VV00 sample (corrected for 2MASS sky coverage) in different magnitude bins. We find that 2MASS is basically 100% complete for $V < 17.5$, and its completeness drops to 50% around $V \sim 18.5$. Therefore, 2MASS would appear to be a good place to find quasars. The main problem, however, is that even when selecting only 2MASS objects away from the Galactic plane that have colors typical of quasars and are away from the stellar locus, and have proper motions (inferred from the distance between 2MASS objects and their USNO A2.0 counterpart) consistent with zero, the stellar contamination is still quite high. We will return to this problem shortly.

3.2. Reference Frame Accuracy

In order to calculate the frame precision (except for VV00) we simulate observations from a mock $R > 14.5$ quasar catalog with an apparent magnitude distribution according to Hartwick & Schade (1990), and including a simple model of Galactic extinction. For the

bright ($R \leq 14.5$) end of quasars we use the actual VV00, since we found it to be complete in that magnitude range. In fact, in this bright part, we remove objects from VV00 that do not have a stellar appearance, although *FAME* could possibly make good measurements of some non-pointlike AGN that exhibit significant nucleus-host contrast. Intrinsic photocenter variation is ignored since it is considerably smaller than the astrometric precision for the great majority of quasars.

In Figure 2, on the left-hand axis, we show the accuracy of the reference frame achieved in the z -direction if different surveys are included and observed by *FAME* to some limiting R magnitude. Next to each line we place labels indicating the approximate number of objects brighter than that point. We use equation (7) to calculate the frame accuracy. The short-dashed line shows what frame accuracy is achieved if only VV00 quasars are used. This is roughly equivalent to asking what quasars *FAME* would be able to observe if it flew now. One can see that the accuracy does not improve much beyond $R = 17$. The VV00 sample includes 1800 quasars to $R = 17$ and produces $\sigma_z = 14.2 \mu\text{as yr}^{-1}$, while including 5000 quasars to $R = 18$ gives only a slightly better accuracy. Better results are obtained when we include the quasars that SDSS will identify by late 2003, plus those from the 2QZ and FBQS surveys. They are shown with the long-dashed line. In this calculation, for regions not covered or inefficiently covered by SDSS, 2QZ and FBQS we keep the VV00 quasars. With these surveys *FAME* can get progressively better result as fainter and fainter quasar candidates are included. At $R = 17$, with 2500 quasar candidates (and assuming they are all actually quasars) one could get $\sigma_z = 13.8 \mu\text{as yr}^{-1}$. If the systematics allow photometry of $R = 19$ objects (71,000 quasars total), the achieved precision becomes $11.6 \mu\text{as yr}^{-1}$. The full line, which we can also consider an ideal case, shows how the quasars detected by *GALEX* could constrain the frame accuracy. We exclude from the calculation *GALEX* quasars within 10° of the Galactic plane, as these will be difficult to distinguish by *FAME*. At $R = 17$, with only 5100 quasars, *FAME* already reaches $\sigma_z = 11.0 \mu\text{as yr}^{-1}$, which improves to $8.6 \mu\text{as yr}^{-1}$ at $R = 18$ and 40,000 quasars, and could ultimately reach $7.1 \mu\text{as yr}^{-1}$ at $R = 19$, using some 270,000 quasars.

As mentioned earlier, one can in principle improve over the situation caused by the possible absence of *GALEX* data and the incomplete sky coverage of SDSS to be available in late 2003 by including quasar candidates selected using 2MASS. However, due to non-negligible stellar contamination in color and proper-motion selected objects from 2MASS, improvements in the frame accuracy are possible only at the cost of including many more objects in the input catalog. In Figure 2 we show with two circled crosses the improvement in frame accuracy by including in the input catalog quasar candidates selected from 2MASS that have R_{USNO} magnitudes less than 17.0 and 18.0 respectively, lie in north and south polar caps with the radius of 60° , centered 10° away from the Galactic poles (in order to

reduce stellar contamination from the bulge), have proper motions consistent with zero, and satisfy the color selection criteria

$$0.2 < B_{\text{USNO}} - J \leq 1.8; \quad J - K_s \geq 0.6 + 0.2(B_{\text{USNO}} - J). \quad (8)$$

This color selection is chosen to maximize quasar detections ($\sim 70\%$ detection efficiency), while keeping the number of stellar contaminants as small as possible. We estimate that $\sim 2\%$ of the candidates selected in this way are actually quasars.

We find that by including 460,000 2MASS candidates to $R_{\text{USNO}} = 17$ one can achieve frame accuracy of $\sigma_z = 11.0 \mu\text{as yr}^{-1}$, and with 960,000 candidates to $R_{\text{USNO}} = 18$ reach $\sigma_z = 10.5 \mu\text{as yr}^{-1}$. It is possible that by adopting some different color criteria, or by avoiding parts of the sky with particularly high stellar contamination, the improvements similar to these can be achieved at a somewhat smaller cost in terms of number of candidates.

Frame accuracy in the x and y directions is 10% better than in the z direction for the *GALEX* sample, regardless of magnitude. For all other surveys the x and y accuracy is 13% better at $R = 16$ increasing linearly to 20% at $R = 19$. Accuracy in the z direction is in all cases the worst, because there are fewer quasars close to the Galactic plane.

We previously mentioned that measuring quasar positions can serve as a check on the systematics of the satellite accuracy. Say, for example, that there is some unmodeled annual effect that changes the basic angle between the two fields of view of *FAME*. This would cause false parallaxes in the certain regions of the sky. One can independently check this is by observing objects with no parallax, like quasars. On the right-hand side axis of Figure 2 we note values of the accuracy of parallax systematics in 1 steradian of the sky obtainable with different quasar samples. (We assume that for the random direction positional accuracy is approximately proportional to z -direction proper motion accuracy. See previous paragraph.) The precision (45 - 75 μas) is adequate to allow detection of systematic effects that are of the order of the mission's best statistical errors.

In addition to astrometry, observing quasars with continuous photometric sampling at an average rate of 1 day $^{-1}$, will permit variability studies with 12% precision per observation at $R = 16$.

4. Kinematics of the Galaxy

4.1. Proper Motion of the Galactic Center and the Motion of the LSR

The proper motion of the Galactic center is the reflex of the Sun's motion around it. Assuming that the compact radio source Sgr A* is at rest with respect to the dynamic

center of the Galaxy, which the huge mass of a black hole associated with it suggests, radio astrometry of Sgr A* by Backer & Sramek (1999) and Reid, Readhead, Vermeulen, & Treuhaft (1999) yields $\mu_{\text{GC}} = -6.2 \pm 0.2 \text{ mas yr}^{-1}$ and $\mu_{\text{GC}} = -5.9 \pm 0.4 \text{ mas yr}^{-1}$, respectively. While not discrepant, these two measurements imply that the proper motion is known to only 5%. By measuring proper motions of great number of bulge stars that are part of the main survey mission ($R < 15$), the statistical error of the mean proper motion will almost vanish, and the ensuing precision of the proper motion of the Galactic center will be limited by the precision with which the reference frame rotation is known. In the previous section we described scenarios in which *FAME* would be able to determine the frame rotation to, say, $7 \mu\text{as yr}^{-1}$. This would therefore allow the proper motion of the Galactic center to be determined to 0.1%, a fifty-fold improvement over the current situation.

Since $\mu_{\text{GC}} = V/R_0$, where the velocity $V = \Theta_0 + V_{\odot}$ is the sum of the rotation speed of the Local Standard of Rest (LSR) and Sun's motion with respect to it, and R_0 is the distance to the Galactic center, the proper motion constrains the ratio of these quantities. Since the *FAME* measurements will practically eliminate statistical uncertainty in μ_{GC} and V_{\odot} , and the uncertainty in R_0 which is currently around 5% might eventually go below 1% (Salim & Gould 1999), *FAME* would be able to determine Θ_0 with 2 km s^{-1} accuracy. Measuring the value of the Milky Way's rotation curve at the Solar circle with such accuracy will improve estimates of its dynamical mass. One will also be able to put constraints on the possible motion of LSR perpendicular to the Galactic plane. Such motion might be the result of the triaxiality of the dark halo. Binney (1995) predicts $\mu_{\text{GC},\perp} = 27 \text{ mas yr}^{-1}$, assuming ellipticity $\epsilon = 0.07$. While today's measurements cannot measure this effect at all, with the frame fixed by faint quasars, *FAME* would be able to measure it with 25% accuracy. Other types of non-axisymmetry, like the Galactic bar, could also be explored to better accuracy in this way.

If the radio measurements of Sgr A* eventually reach comparable precision, it will be possible to test with high precision the premise that Sgr A* represents the dynamical center of the Galaxy by comparing the Sgr A* proper motion to the mean proper-motion of bulge stars measured by *FAME*. In the direction perpendicular to the Galactic plane, this test would be essentially free of possible systematic effects.

4.2. Rotation of the Galactic Halo

Studies of the Galactic halo shed light on the formation of our galaxy. The kinematics of the stellar halo are an important indicator of the formation mechanisms involved. Some of the more recent studies that derive the halo velocity ellipsoid in the inner halo include

Layden et al. (1996) who used low-metallicity RR Lyraes, and Gould & Popowski (1998) who used low-metallicity RR Lyraes as well as other low-metallicity stars. Gould & Popowski (1998) derive a halo rotation in prograde direction of $34.3 \pm 8.7 \text{ km s}^{-1}$ with respect to the Galactic frame. This estimate, which assumes that the Sun’s velocity in the Galactic plane is 232 km s^{-1} in the prograde direction, applies to halo stars within 3 kpc.

FAME will be able to greatly improve the range, the resolution and the accuracy of the halo velocity ellipsoid, thus allowing one to see any gradient in motion. *FAME* will be able to do this by observing many faint blue horizontal branch stars in various directions of the sky. Horizontal branch stars are especially favorable for mapping purposes as their nearly constant luminosity permits a relatively precise estimate of their distances.

Candidate blue horizontal branch stars (BHB stars) can be effectively selected from multi-band photometry. This was recently demonstrated by Yanny et al. (2000) using SDSS $u'g'r'$ photometry. Their study showed that A-colored stars (A-stars) trace huge substructures in the halo. Unfortunately, other types of blue stars, those with main sequence gravity (mostly field blue stragglers (BSs)), have similar colors as BHB stars, and it is not clear whether distinguishing between these two populations can be done based on photometry alone. Mixing these two types of stars that have very different absolute magnitudes (and with BS luminosities likely having a strong metallicity dependence as well) makes it difficult to use them as distance indicators. One certain way of distinguishing any individual star is by measuring the widths of Balmer lines that indicate surface gravity (BHB stars have lower surface gravity and narrower lines). However, spectroscopy will not be available in the majority of cases, and we must consider other methods. The stars of the two population with same apparent magnitudes lie at different distances, so they will on average exhibit different proper motions. It is this feature that we will use to distinguish between BS and BHB-star populations.

BHB stars with $R < 15$ will already be included in the *FAME* input catalog. In the 1/2 of the north polar cap for which SDSS data will be available one can employ color criteria similar to those used by Yanny et al. (2000). Selecting stars with $15 < r^* < 18$ (for blue stars SDSS r^* is quite close to R), and with dereddened colors

$$-0.3 < g^* - r^* < 0.1 \quad 0.8 < u^* - g^* < 1.5 \quad (9)$$

we derive a surface density of A-stars in the $\sim 500 \text{ deg}^2$ of SDSS Early Release Data (EDR) of $\sim 4.2 \text{ deg}^{-2}$. This implies that approximately 20,000 BHB star candidates will come from SDSS. For the rest of the northern cap and the entire southern cap, one can try to retrieve BHB candidates from some other all-sky catalog. We perform this exercise using USNO-A2.0, although the Guide Star Catalog 2 (GSC-2), which will have better calibrated photometry, will be better suited. Since in the case of USNO-A2.0 we have at our disposal

only two-band photometry which is quite crude (color error of ~ 0.4 mag), we need to estimate the efficiency of getting A-star candidates given some level of contamination from the many times more numerous turn-off stars. To do this we matched SDSS EDR A-stars to USNO-A2.0 objects and identified them on the USNO-A2.0 color-magnitude diagram (CMD) of all stars within the SDSS EDR sky coverage. SDSS selected A-stars in this CMD lie on the blue side, as expected, but are not clearly separated from the turn-off star locus. Since USNO-A2.0 provides only single color on which to base the selection, the blue portion of the USNO-A2.0 CMD also contains white dwarf and quasar contaminants, as well as turn-off stars. In the case of SDSS selection these quasars and white dwarfs were eliminated using the $u^* - g^*$ color. Although in the present context WDs and QSOs are considered as contaminants, including them in the input catalog is useful for other aspects of this project. As stated previously, QSOs can be distinguished by their K -band excess, while WDs will stand out by their much higher proper motions.

The locus of both the turn-off stars and the SDSS selected A-stars in the USNO-A2.0 CMD is tilted with a slope corresponding to the line,

$$B_{\text{USNO}} - R_{\text{USNO}} = a - 0.15R_{\text{USNO}}, \quad (10)$$

where a is the zero point of the line. Now we can count the number of $15 < R_{\text{USNO}} < 18$ USNO-A2.0 stars left (blue-ward) of this line as we shift this line red-ward, and at the same time noting how many USNO matches to SDSS selected A-stars are included in the region to the left of the line. As we move red-ward, both the number of real (SDSS selected) A-stars and the number of USNO-A2.0 A-star candidates will increase. We find that the ratio of USNO-A2.0 A-star candidates to SDSS A-stars remains constant for $a < 2.4$, but that the turn-off contamination increases rapidly further red-ward of this point. For $a < 2.4$ we find the ratio of USNO candidates to SDSS A-stars to be 12. Such selection retrieves 54% of SDSS selected A-stars. To summarize, if this selection is applied to $15,000 \text{ deg}^2$ of the northern and southern caps not covered by SDSS, one will end up with 340,000 candidates that will contain 28,500 actual A-stars. Note again that many of these ‘contaminants’ will be QSOs and WDs which one would want anyway.

In the case that the *GALEX* UV sky survey becomes available, we would be able to eliminate turn-off contaminants in USNO-A2.0 selected A-star candidates. Alternatively, one can use *GALEX* to select A-star candidates and then match them in USNO-A2.0 (or better yet GSC-2).

We now come to the question of distinguishing A-stars as either BHB stars or BSs, using proper motions from *FAME*. For simplicity, we will assume that all A-stars are located exactly in the direction of the Galactic pole, so that only two of the three components of the motion are expressed. In one direction, let us call it y , we will then see the rotational

motion around the center of the Galaxy. The velocity corresponding to this motion is approximately 200 km s^{-1} , and the velocity dispersion in this direction according to Gould & Popowski (1998) is 109 km s^{-1} . In the perpendicular direction (x), parallel to Sun–Galactic center vector, we will assume no bulk motion, and the Gould & Popowski (1998) velocity dispersion of 160 km s^{-1} .

At each apparent magnitude both BHB stars and BSs are sampled, but their ratio, even if constant in a given volume, is not independent of apparent magnitude. If we assume, as for example implied by Yanny et al. (2000), that in a given volume the field BSs outnumber field BHB stars 2:1, and that both populations fall off with Galactocentric distance as $r^{-3.5}$, then from our vantage point 8 kpc from the center, at any given magnitude we will sample BSs at a different Galactocentric distance than BHB stars, and the magnitude bin will correspond to different volumes for the two types of stars because of different heliocentric distances. Thus at $R = 15$ we find $N_{\text{BS}}/N_{\text{BHB}} = 0.17$, but at $R = 19$ the ratio is 2.3. Other values can be deduced from Table 1.

Next we use Monte Carlo techniques to simulate observations of all A-stars that one hopes to select using SDSS and USNO-A2.0, as previously described. We do this for $R = 15, 16, 17, 18$, and 19. For each magnitude bin ($R \pm 0.5$) we first estimate the number of BHB stars and BSs that *FAME* will detect in that bin (given in Table 1), then to BHB stars we assign an absolute magnitude drawn randomly from $M_R = 0.8 \pm 0.15$, while to BSs we assign absolute magnitudes distributed as $M_R = 3.2 \pm 0.5$, where the dispersion is meant to reflect the range of absolute magnitudes at a given color. This will determine the distance to that star. Then each star is assigned two components of physical velocity drawn from the halo velocity distribution described earlier in this section. Using the distance, we convert this velocity into a true proper motion. The observed proper motion is then obtained by adding in a measurement error based on the *FAME* accuracy σ_μ from § 2.1.

Since at any given magnitude BSs lie three times closer than BHB stars, in each apparent magnitude bin there will be two peaks in proper motion, corresponding to BSs and BHB stars. Because of proximity and because of a greater spread of absolute magnitudes, the distribution of proper motions corresponding to BSs will be wider at a given magnitude than that of BHB stars. It is the position of the peak of BHB stars proper motion distribution in y -direction that will yield the halo rotational velocity. To find out how well this peak can be determined in the face of BS contamination, we calculate errors in fitting 2-dimensional Gaussians to each of the two peaks. Each Gaussian is defined by six parameters – two for the x and y center of the peak, three for two diagonal (σ_{xx}, σ_{yy}), and one off-diagonal (σ_{xy}) term in the covariance matrix describing peak widths, and one corresponding to the number of stars (amplitude). We calculate the errors of these parameters from our simulated

measurements.

The results are summarized in Table 1. The second column lists the distance of BHB stars of magnitude R , which is given in the first column. The third and fourth columns list the number of BHB stars and BSs that we expect *FAME* to measure in the two caps ($|b| > 30^\circ$). The next two columns list the errors that we derive for the position of the BHB proper motion peak, and columns 7 and 8 list estimates of the uncertainty of the BHB stars velocity dispersion along y and x directions. The final column, derived from columns 2 and 5, shows the expected error in the stellar halo rotation velocity. In Figure 3 we present σ_{rot} as a function of R or d . One can see that within 20 kpc *FAME* achieves a precision of halo rotation measurement of $\lesssim 2 \text{ km s}^{-1}$ if the data are binned in 1-mag steps. Better spatial sampling (resolution) can be achieved by choosing smaller bins, but with correspondingly larger errors. At distances to ~ 30 kpc quite good estimates of stellar halo rotation can still be made. Only farther out do the measurement errors and the preponderance of BSs of same magnitude as the BHB stars preclude obtaining a useful result. Note that here we assume that the BHB stars' luminosity will be very well determined locally by *FAME*'s trigonometric parallaxes, and that this luminosity does not depend on distance from the plane. To get motions relative to the Galactic frame, it will of course be necessary to subtract the Sun's circular velocity, which will have been determined as described in §4.1.

A more sophisticated analysis would show that the halo rotation can be mapped in two dimensions, instead of one as outlined here. Such probing of the halo potential would place more constraints on the dark halo models. Additional information on the still debated shape of the dark matter halo (flatness [Olling & Merrifield 1998, 2001] and triaxiality) will be gleaned from the three-dimensional distribution of stars determined to be BHB stars from *FAME* proper motions. An effect that might introduce systematic error in distances and thus the velocities is if BHB stars change in luminosity (due to age and metallicity effects) as we move above the plane. This problem might be eliminated by imposing an axial symmetry—we would require v_{rot} to be constant at a given Galactocentric radius, regardless of the direction. Such a treatment requires an analysis that is beyond the scope of this paper.

In the above analysis we have used BHB stars to probe halo kinematics and considered BSs as a contaminating factor. We note that with the halo motion determined by BHB stars, the measured proper motions of BSs can be used to derive their luminosity calibration and distribution of metallicities.

4.3. Substructure in the Galactic Halo

Recently discovered clumps of RR Lyrae stars (Ivezić et al. 2000), and A-colored stars (Yanny et al. 2000) in the halo indicate that the Galaxy formation mechanism might be more complex than previously envisaged, and that accretion or merging of small galaxies might have played a crucial role. Some models even suggest that all halo stars come from disrupted satellite galaxies. The structures found by Yanny et al. (2000) lie at Galactocentric distances of 30 to 50 kpc, and extend over many kiloparsecs. The structures are seen as overdensities of BHB stars and BSs, i.e., only positional information is used. The third coordinate, the distance, is compromised because of difficulties with BHB/BS distinction, leading to smearing of the features. Besides being clumped in space, the stars originating from the same disrupted satellite should cluster in velocity space as well. In fact, the velocity information is conserved much better than the spatial information, and it is possible to associate stars that are widely separated on the sky and that have mixed spatially with other streams. Helmi & White (1999) have shown that 10 Gyr after a merging event the spatial distribution of stars in the halo will be very smooth, while hundreds of halo streams, strongly ($\sigma_v < 5 \text{ km s}^{-1}$) clustered in velocity space will still be present.

FAME observations will yield two components of velocity that can be used to detect substructure in the halo. The old halo streams predicted by Helmi & White (1999) will require local samples of subdwarfs. The best sensitivity for detecting such streams comes from analyzing the proper motions of G-subdwarfs (halo turn-off stars) which are bright and numerous. Helmi & White (1999) suggest that the velocity accuracy needed to resolve individual streams is $< 5 \text{ km s}^{-1}$, but that they will be detectable at several times that accuracy. We believe that such studies will be possible with stars selected as part of the *FAME* main survey ($R < 15$). Including fainter stars might not be useful as the velocity accuracy would be limited by inaccurate distances. This is indicated by Helmi & de Zeeuw (2000) who find that *FAME* will be able to distinguish 15% of the nearby halo streams. Their sample of halo giants is limited by parallax errors to $V < 12.5$, and the velocity measurements are augmented with an assumed ground-based radial velocity survey.

Bigger structures (tidal streams and remnants of recently disrupted satellites) might be detectable in the $R > 15$ BHB star sample discussed previously. The specific structures found by Yanny et al. (2000) may be too distant to be detected by *FAME*, yet their survey covers only 1% of sky, so more nearby clumps are likely to be present in the rest of the sky. To find them one should aim at $\sim 20 \text{ km s}^{-1}$ accuracy per star. With the good photometric parallaxes achievable for BHB stars, substructure mapping might be possible to distances of 10 kpc (corresponding to $R_{\text{BHB}} \approx 16$).

4.4. Proper Motion of LMC, SMC, Dwarf Spheroidals and Globular Clusters

Proper motions of the Magellanic Clouds, dwarf spheroidal galaxies and globular clusters add to our knowledge of the kinematics of these objects and the extent and properties of Milky Way’s dark matter halo (e.g Wilkinson & Evans 1999; Kochanek 1996). *FAME* will in some cases observe proper motions of bright ($R < 15$) stars in these systems, thus allowing the proper motion of the entire system to be determined. For the LMC and SMC, at least, the accuracy will only be limited by the accuracy of the reference frame. Hence, a precise determination of reference frame rotation using quasars, as described in §3, will again be of importance. Let us illustrate this with the case of the LMC. Gould (2000) has shown that a kinematic distance to the LMC can be obtained independent of any distance calibrators such as RR Lyraes or Cepheids. The method requires a measurement of the proper motion of the LMC. Using *FAME* observations of ~ 8600 $13 < V < 15$ LMC stars, Gould (2000) estimates that the proper motion of the LMC can be determined to $2 \mu\text{as yr}^{-1}$, or 0.2% accuracy. However, this unprecedented accuracy is limited by frame accuracy, and would be compromised if only $R < 15$ quasars were used to define the frame.

5. Faint Nearby Stars

5.1. Late-M and L Dwarfs

In recent years there has been a major breakthrough in the discovery and study of late-type stars and substellar objects (brown dwarfs). Wide-area sky surveys, that either go much fainter than the previous ones (SDSS), or image the sky in the near-infrared where these cool stars emit most of their energy (2MASS, DENIS), allow for the first time a great number of these objects to be discovered. These discoveries led to the introduction of two new spectral classes: L dwarfs that are cooler than the latest M dwarfs and some of which might have substellar mass, and T dwarfs that exhibit methane absorption and which are certainly substellar. Currently, over 100 L dwarfs have been found, and some two dozen T dwarfs (Burgasser et al. 2002; Leggett et al. 2002; Kirkpatrick et al. 2000).

Accurate distances are a key factor in understanding the structure and evolution of these objects. Besides establishing luminosity calibration, distances would allow better constraints on other key parameters like the radius and the temperature. Distances are currently available for about 20 L dwarfs, and a few T dwarfs. In some cases a precise distance is known only because the object is a companion to a star with a measured trigonometric parallax. Distances will also help constrain the luminosity function of these objects.

Even for the more easily discovered late M dwarfs, the faint end of the main sequence ($V - I > 3$) is defined with the trigonometric parallaxes of only some 30 stars, mostly coming from the USNO CCD parallax program (Monet et al. 1992). This is too few to accurately describe the differences in absolute magnitudes of different populations of stars.

One of the already recognized mission goals of *FAME* is to refine the absolute magnitude calibration in the entire HR diagram, including the faint main sequence stars. However, selecting only $R < 15$ stars will leave unmeasured many stars for which good ($< 10\%$ accuracy) parallaxes are within the reach of *FAME*, with the ratio of unobserved to observed stars getting worse as one goes further down the main sequence.

In Figure 4 we compare the number of stars for which *FAME* will be able to measure parallaxes with $< 10\%$ errors if no magnitude limit is imposed, compared to the number of such stars brighter than $R = 15$. Our first bin is dM5.5 stars (equivalent to $M_V = 14$). There are intrinsically brighter stars (late K and early M dwarfs) for which including $R > 15$ stars would also produce many additional good parallaxes. However, the number of such stars with $R < 15$ is already high enough to allow calibration at the level of their intrinsic scatter. In calculating the number of stars in Figure 4 we use current estimates from the literature for the colors, magnitudes, and space densities for late-M, L and T dwarfs, coupled with *FAME* astrometric precision. The numbers for L dwarfs are less certain (by a factor of two) because of their poorly known number densities. Since the stars fainter than $R = 15$ must be deliberately selected to be included as nearby star candidates, and this selection might be difficult close to the Galactic plane, our estimate is based on the assumption that M dwarfs will be selected only if their Galactic latitude satisfies $|b| > 20^\circ$. On the other hand, we assumed that L dwarf candidates will be followed up and confirmed in all regions of the sky.

For dM5.5 stars, discarding the $R = 15$ magnitude limit augments the number of parallaxes from 600 to 4000 by extending the volume probed from 30 to 64 pc. For the very latest M-dwarfs (M7 to M9.5) one will obtain 500 measurements, compared to only 16 for $R < 15$. Finally about 5 L dwarfs are present in the $R > 15$, $\sigma_\pi/\pi < 0.1$ sample, whereas the $R < 15$ limit excludes all L dwarfs. It is obvious that, except for L dwarfs, which are very faint and whose parallaxes are possibly better determined by other means (ground-based campaigns, space telescopes), accepting this magnitude-limit-free selection leads to great improvements in calibrating low-mass stars. We also find that T dwarfs are outside of reach of *FAME*, although a few lower precision measurements could possibly be made.

While most of the nearby L and T dwarfs will be found and confirmed by dedicated searches, late M dwarfs need to be selected from some catalog. Fortunately, 2MASS will contain all the late M dwarfs that *FAME* can observe. We estimate the number of $M_V > 14$

candidates by running a search through the 2nd Incremental Release of 2MASS PSC. We use the following search criteria: $H - K > 0.3$, $J - H > 0.3$ and $R_{\text{USNO}} - K_s > 3.5$ (or no USNO detection) to select late M dwarfs based on color; $J - K_s \leq 4/3(H - K_s) + 0.25$ to eliminate M giants (Gizis et al. 2000); $J \leq 14.5$ to ensure selection of nearby objects, and $R_{\text{USNO}} > 15$ to exclude stars already in the *FAME* main survey list. The search is further restricted to $|b| > 20^\circ$ to exclude contaminants in the Galactic plane. We find the average density of candidates to be 2.3 deg^{-2} , implying 64,000 total candidates, which is a modest addition to the *FAME* input catalog. In 1/5 of this area SDSS photometry will also be available which will permit refinement of the selection. The selection can be further augmented with GSC-2, which will contain photometry similar to I band. Any contaminants in this sample will at the end be obvious from the *FAME* parallax measurements themselves.

5.2. White Dwarfs

White dwarfs are one of the most numerous stellar populations in our neighborhood. Therefore they represent obvious targets for getting precise distances. A large sample of parallaxes would allow one to study the white dwarf mass function. The mass of a white dwarf is related to the mass of the progenitor and can thus serve as an indicator of the IMF at different epochs. Current measurements of the mass function are still somewhat controversial both in terms of the peak mass (estimates range from $0.48M_\odot$ to $0.72M_\odot$) and also concerning the width of the mass function (for recent results see Silvestri et al. 2001). At a given temperature (or color), WDs exhibit a range of absolute magnitudes reflecting a range of radii, since the absolute magnitude is then primarily a function of the white dwarf's radius. Then the mass-radius relation, which is very well determined theoretically, allows one to find the masses. Other methods of getting masses either rely on a few binary systems or are of low precision (gravitational redshift). Obtaining luminosities of the coolest white dwarfs is also useful for testing the predicted cooling scenarios.

Currently ~ 200 precise (accuracy better than 10%) trigonometric parallaxes of white dwarfs are known (McCook & Sion 1999). Using the white dwarf luminosity function from Liebert, Dahn, & Monet (1988) and our estimates of *FAME* parallax precision, we estimate that the *FAME* survey of $R < 15$ stars will produce $< 10\%$ parallaxes of 400 white dwarfs. However, as in the case of late-M and L dwarfs, one can increase this number by including in the input catalog objects fainter than $R = 15$. Then the total number of white dwarfs with precise parallaxes measured by *FAME* rises to 2400, i.e., a six-fold increase. This increase is accentuated for fainter white dwarfs, as can be seen in Figure 5. For example, for $M_V > 13$ ($T \lesssim 8500$ K) the increase with respect to $R < 15$ sample is thirteen-fold. Such

numbers would allow mass functions to be constructed as a function of age, and for different atmospheric compositions.

The magnitude limit for 10% parallaxes will range from $R = 15.5$ for the bluest white dwarfs ($M_V = 9.5$), to $R = 17.6$ for the reddest ($M_V = 16.5$). These faint WDs must first be selected and then added to the input catalog. Currently known white dwarfs account for $\lesssim 40\%$ of the expected $R > 15$ sample, based on white dwarfs with photometric information from McCook & Sion (1999). The most efficient way of selecting white dwarfs is by using an all-sky proper motion catalog. Then, the white dwarfs are selected from a reduced proper-motion diagram in which the reduced proper motion, $H_m = m + 5 \log \mu + 5$, is plotted against color. For a stellar population with approximately the same transverse velocities, the proper motion becomes a proxy for the distance, and the reduced proper motion a proxy for the absolute magnitude. Because the white dwarfs are separated by ~ 10 mag from the main sequence, they will stand out in a reduced proper-motion diagram by the same amount, since the two populations have on average the same transverse velocities. For redder white dwarfs, there will be some contamination from subdwarfs, since due to their greater velocity these stars will move down into the white dwarf region. However, even if some subdwarfs ‘contaminate’ the white dwarf observing list, these stars will be of considerable interest in their own right. The only currently available all-sky proper motion catalog that contains faint stars, the Luyten (1979, 1980) NLTT catalog, has a proper motion cutoff that is too high to include most of the white dwarfs with typical disk velocities that lie within the volume accessible to *FAME*. Thus, it will be necessary to draw white dwarf candidates from the yet to be released GSC-2 or USNO-B that will include all detectable proper motions with typical accuracy of 5 mas yr^{-1} . This will be precise enough to select even the farthest WDs that produce 10% parallax measurement, since they typically move at 40 mas yr^{-1} . In the part of the sky observed by SDSS, hot ($B - V < 0.3$) white dwarf candidates can be selected solely based on their very blue color in *all* SDSS bands (as distinct from other blue objects like the quasars and A-type stars, see Fan 1999), while SDSS photometry of red candidates from GSC-2/USNO-B will be good enough to distinguish subdwarfs from WDs. GSC-2/USNO-B white dwarf candidates can additionally be cross-correlated with *GALEX* UV sources, assuming that the *GALEX* survey is complete by the time required to define the input catalog. Some nearby white dwarfs might also end up in the input catalog as ‘contaminants’ from other projects suggested here (when selecting quasars and blue horizontal branch stars). Generally, we do not expect the white dwarf candidates to represent a significant increase in the input catalog size. It will be useful for spectroscopic follow-up to commence as soon as candidate nearby white dwarfs are identified. Besides offering spectroscopic confirmation, spectroscopy is necessary to establish white dwarf atmosphere composition that in turn allows parallax data to be interpreted correctly.

5.3. Planetary and Brown Dwarf Companions of M Dwarfs

Here we examine how adding faint ($R > 15$) M dwarfs to the *FAME* input catalog can affect its sensitivity to brown dwarfs and planets. For completeness, we show *FAME*'s sensitivity to companions of earlier type dwarfs as well. To perform this calculation we adopt the vertical disk profile of Zheng et al. (2001) (Table 3, all data, CMR-2, sech^2 model), and adopt their (CMR-2) M dwarf luminosity function (LF) as well. For earlier type stars we use the LF of Bessell & Stringfellow (1993). Note that the Zheng et al. (2001) LF is uncorrected for binaries which is appropriate because most M dwarfs that are companions of brighter primaries will not be individually resolved by *FAME*.

Figure 6 shows the number of stars whose companions of a given mass would be detectable by *FAME*. It specifically assumes a 20% mass measurement threshold, and an orbital period of $P = 5$ yr. The effect of requiring 10σ detections can be approximately gauged by displacing all the curves by 0.3 dex to the right. For shorter periods, one should displace the curves to the right by $(2/3) \log(5 \text{ yr}/P)$. For example, for $P = 2.5$ yr, the curves should be displaced by 0.2 dex. Figure 6 illustrates that the major effect of including faint M dwarfs is to enhance sensitivity to brown dwarf companions of late M dwarfs. For companions just below the hydrogen burning limit, there is an order of magnitude improvement. Note that *FAME* will be sensitive to Jupiter mass companions of 1300 M stars and to 10-Jupiter mass companions of 45,000 M stars, and of an even larger number of G and K stars. However, these remarkable sensitivities will not be significantly improved by inclusion of faint stars.

5.4. Miscellaneous Stars

Our targeted search to include late M dwarfs and white dwarfs should ensure that most such nearby objects are included, however there is a possibility that some will be missed. Therefore, and also for the sake of ensuring a volume-complete sample of the nearest stars (within 25 pc), one should make sure that all objects from the Catalogue of Nearby Stars (Gliese & Jahreiss 1991, CNS3) are in the input catalog. Furthermore, it will be useful to include the complete NLTT. Besides still representing a reservoir of new nearby stars (Scholz, Meusinger, & Jahreiss 2001), NLTT contains many stars with intrinsically high space velocities – subdwarfs, and some halo white dwarfs. The luminosity calibration and true space velocity of these objects is of great interest in many Galaxy evolution studies. Finally, a few other interesting objects found in other surveys (again, like high-velocity white dwarfs) should be included. All of these targets will comprise a negligible fraction of the *FAME* input catalog. In fact, there are relatively few specially selected and catalogued stars (of any magnitude), and all of them will most likely end up in the *FAME* input catalog (D.

Monet 2001, private communication).

6. Impact on Main Survey

Depending on which sky surveys will be available several years from now, and on exactly which of the various selection strategies that we have elaborated were adopted, the faint samples discussed above would total of order $\mathcal{O}(10^6)$ objects, or about 2.5% of the *FAME* catalog. Since *FAME* is fundamentally limited by data transmission rate, these catalog entries would come at the expense of the magnitude-limited sample, e.g., by reducing the magnitude limit by 0.03 mag. This would not significantly affect any of *FAME*'s primary science goals.

7. *DIVA* and *GAIA*

As discussed in § 1.2 and § 2.1, the characteristics of *DIVA* are close enough to those of *FAME* that the methods and arguments presented here can be applied directly to *DIVA*. Indeed, if the constants c_{RN} in equations (4) and (5) were the same, the entire analysis of *FAME* could be applied directly to *DIVA* simply by rescaling the errors (by a factor 4.0 for parallaxes and 6.4 for proper motions). Since the read-noise limit sets in 0.64 mag brighter for *DIVA* than *FAME*, pushing beyond the magnitude limit yields slightly less additional science. Nevertheless, qualitatively the effect is the same.

While the methods presented here can ultimately be used to choose faint targets for *GAIA*, it is not practical to do so at the present time, primarily because the luminosity functions of the relevant target populations are not sufficiently well understood. For example, one could in general advocate observing quasars fainter than $V = 20$ *GAIA* limit in order to improve the reference frame. However, the net frame error from observing a flux-limited sample of quasars scales as

$$\sigma_{\text{frame}}^{-2} \propto \int_{F_{\text{lim}}}^{\infty} dF [\sigma(F)]^{-2} \Phi(F), \quad (11)$$

where $\Phi(F)$ is the quasar LF as a function of flux. Figure 2 shows that there is a substantial improvement in the *FAME* frame when going from $R = 18$ to $R = 19$, even though the readnoise limit applies, $\sigma(F) \propto F^{-1}$. This is because the LF is very steep, $\Phi \propto F^{-2.8}$, so the integrand in equation (11) scales as $\propto F^{-0.8} dF$. The LF is believed to flatten considerably (index change ~ 1) at $R \sim 19$ (Hartwick & Schade 1990) which, if true, would virtually eliminate the value of going to still fainter quasars. However, this break in the LF is based

largely on photographic data and occurs just at the magnitude at which the quasars fall below the sky. It therefore may be subject to revision when wide-area CCD data come in from SDSS. On the other hand, if *GAIA* ultimately manages to operate in the photon-limited (rather than currently foreseen readnoise-limited) regime, this would approximately compensate for the break in the slope. Hence there is simply too much uncertainty in both the sample characteristics and the mission characteristics to make a reliable judgement on the usefulness of this type of extension. Similar remarks apply to pushing *GAIA* beyond its magnitude limit in pursuit of L and T dwarfs, halo white dwarfs, and indeed any class of objects that one might contemplate.

It should be noted that unlike *FAME*, *DIVA* and *GAIA* do not use input catalogs, but cut off faint stars using an on-board photometer. Nevertheless, in those cases, like in the case of *FAME*, a list of faint objects that should not be cut off should be produced in advance and provided to a satellite.

8. Conclusions

Hipparcos added faint stars to its observing list that were approximately equal in number to the catalog’s magnitude-limited component, thereby permitting a wide variety of scientific investigations that would not otherwise have been possible. Future astrometric missions can also dramatically augment their science capability by adding targets beyond their magnitude limit. We have specifically analyzed the potential of *FAME* in this regard, and found that the addition of $\mathcal{O}(10^6)$ targets (2.5% of the total) can improve the precision of the reference frame by a factor ~ 2.5 , yield precise (2 km s^{-1}) measurements of halo rotation out to 25 kpc, greatly improve the proper-motion measurements of Galactic satellites, and increase the samples of L dwarfs, M dwarfs, and white dwarfs with good parallaxes by an order of magnitude. We have shown that assembling the various target lists required to make these observations is not trivial, but have presented viable approaches to selection in each case.

The methods that we have presented could easily be applied to *DIVA*. Application to *GAIA* should be deferred until closer to launch when both the mission characteristics and the potential target characteristics are better understood.

This publication makes use of catalogs from the Astronomical Data Center at NASA Goddard Space Flight Center, VizieR Catalogue Service in Strasbourg, and data products from the Two Micron All Sky Survey, which is a joint project of the University of Massachusetts and the Infrared Processing and Analysis Center/California Institute of Technology, funded by the NASA and the NSF. It also uses services of SDSS Archive, for which

funding for the creation and distribution has been provided by the Alfred P. Sloan Foundation, the Participating Institutions, the National Aeronautics and Space Administration, the National Science Foundation, the U.S. Department of Energy, the Japanese Monbukagakusho, and the Max Planck Society. The SDSS Web site is <http://www.sdss.org/>. SDSS is a joint project of The University of Chicago, Fermilab, the Institute for Advanced Study, the Japan Participation Group, The Johns Hopkins University, the Max-Planck-Institute for Astronomy (MPIA), the Max-Planck-Institute for Astrophysics (MPA), New Mexico State University, Princeton University, the United States Naval Observatory, and the University of Washington. This work was supported in part by Jet Propulsion Laboratory (JPL) contract 1226901.

REFERENCES

Backer, D. C. & Sramek, R. A. 1999, *ApJ*, 524, 805

Barkhouse, W. A. & Hall, P. B. 2001, *AJ*, 121, 2843

Bessell, M. S. & Stringfellow, G. S. 1993, *ARA&A*, 31, 433

Binney, J. 1995, *IAU Symp.* 166: Astronomical and Astrophysical Objectives of Sub-Milliarcsecond Optical Astrometry, 166, 239

Boyle, B. J., Shanks, T., Croom, S. M., Smith, R. J., Miller, L., Loaring, N., & Heymans, C. 2000, *MNRAS*, 317, 1014

Burgasser, A. J. et al. 2002, *ApJ*, 564, 421

European Space Agency (ESA). 1997, The Hipparcos and Tycho Catalogues (SP-1200; Noordwijk: ESA)

Fan, X. 1999, *AJ*, 117, 2528

Gizis, J. E., Monet, D. G., Reid, I. N., Kirkpatrick, J. D., Liebert, J., & Williams, R. J. 2000, *AJ*, 120, 1085

Gliese, W., & Jahreiss, H. 1991, Preliminary Version of the Third Catalogue of Nearby Stars (Astron. Rechen-Institut, Heidelberg)

Gould, A. 2000, *ApJ*, 528, 156

Gould, A. & Popowski, P. 1998, *ApJ*, 508, 844

Hartwick, F. D. A. & Schade, D. 1990, *ARA&A*, 28, 437

Helmi, A. & de Zeeuw, P. 2000, *MNRAS*, 319, 657

Helmi, A. & White, S. D. M. 1999, *MNRAS*, 307, 495

Ivezić, Ž. et al. 2000, *AJ*, 120, 963

Kirkpatrick, J. D. et al. 2000, *AJ*, 120, 447

Kochanek, C. S. 1996, *ApJ*, 457, 228

Layden, A. C., Hanson, R. B., Hawley, S. L., Klemola, A. R., & Hanley, C. J. 1996, *AJ*, 112, 2110

Leggett, S. K. et al. 2002, *ApJ*, 564, 452

Liebert, J., Dahn, C. C., & Monet, D. G. 1988, *ApJ*, 332, 891

Luyten, W. J. 1979, 1980, New Luyten Catalogue of Stars with Proper Motions Larger than Two Tents of an Arcsecond (Minneapolis: University of Minnesota Press)

McCook, G. P. & Sion, E. M. 1999, *ApJS*, 121, 1

Monet, D. G., Dahn, C. C., Vrba, F. J., Harris, H. C., Pier, J. R., Luginbuhl, C. B., & Ables, H. D. 1992, *AJ*, 103, 638

Monet, D. G. 1998, American Astronomical Society Meeting, 193, 112003

Murison, M. 2001, <http://arnold.usno.navy.mil/murison/FAME/ObservationDensity/AstrometricErrors4.html>

Olling, R. P. 2001, USNO Memorandum FTM2001-14, <http://ad.usno.navy.mil/~olling/FAME/FTM2001-14.ps>

Olling, R. P. & Merrifield, M. R. 2001, *MNRAS*, 326, 164

Olling, R. P. & Merrifield, M. R. 1998, *MNRAS*, 297, 943

Reid, M. J., Readhead, A. C. S., Vermeulen, R. C., & Treuhaft, R. N. 1999, *ApJ*, 524, 816

Richards, G. T. et al. 2001, *AJ*, 122, 1151

Salim, S. & Gould, A. 1999, *ApJ*, 523, 633

Scholz, R.-D., Meusinger, H., & Jahreiss, H. 2001, *A&A*, 374, L12

Silvestri, N. M., Oswalt, T. D., Wood, M. A., Smith, J. A., Reid, I. N., & Sion, E. M. 2001, *AJ*, 121, 503

USNO 1999, FAME Concept Study Report, USNO: Washington, DC (available at <http://www.usno.navy.mil/FAME/publications>)

Veron-Cetty, M. P. & Veron, P. 2000, ESO Scientific Report

White, R. L. et al. 2000, *ApJS*, 126, 133

Wilkinson, M. I. & Evans, N. W. 1999, *MNRAS*, 310, 645

Yanny, B. et al. 2000, *ApJ*, 540, 825

York, D. G. et al. 2000, AJ, 120, 1579

Zheng, Z., Flynn, C., Gould, A., Bahcall, J. N., & Salim, S. 2001, ApJ, 555, 393

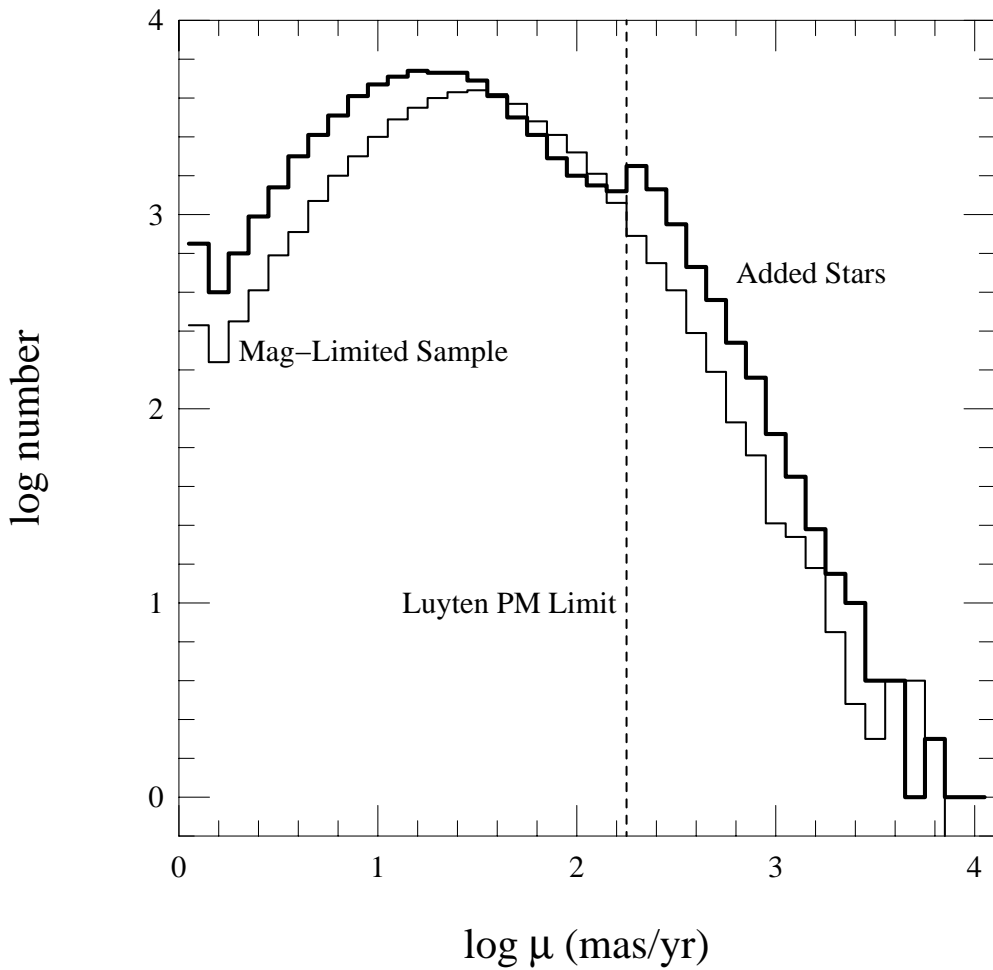


Fig. 1.— Number of *Hipparcos* stars lying within (*solid histogram*) or beyond (*bold histogram*) the *Hipparcos* magnitude limit as a function of their measured proper motion, μ . (This mag limit ranges from $V = 7.3$ to $V = 9.0$, depending on Galactic latitude and spectral type.) The effect of adding stars drawn from the Luyten (1979, 1980) NLTT catalog with its proper-motion limit of $\mu = 180 \text{ mas yr}^{-1}$ (*dashed line*) is clearly visible. Many of these stars are dim (and hence close) and therefore have good parallaxes. However, the majority of added stars have very small ($\sim 15 \text{ mas yr}^{-1}$) proper motions, and hence barely measurable parallaxes. Like *Hipparcos*, future astrometry missions can profit by adding both classes of stars to their otherwise magnitude-limited catalogs.

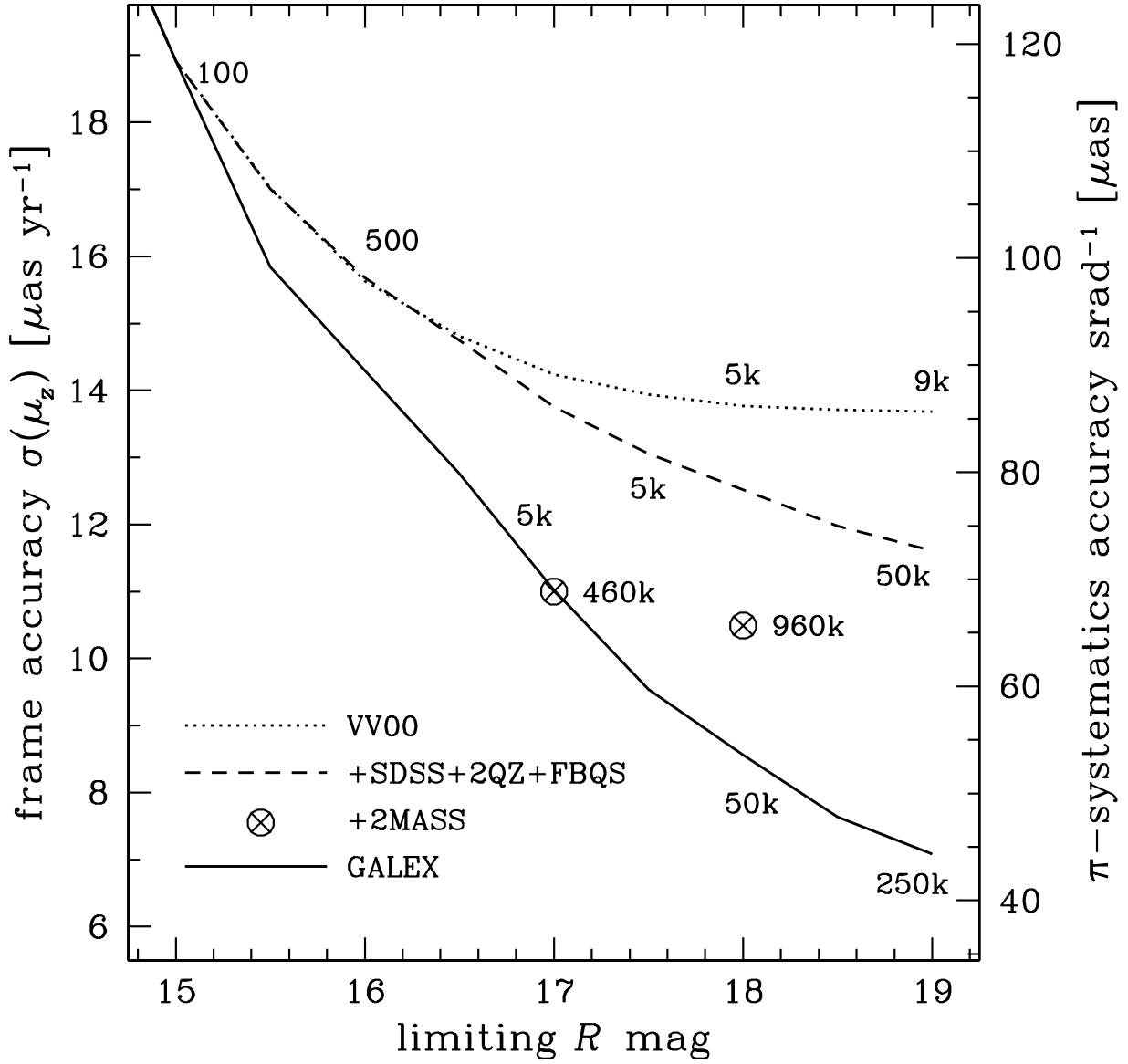


Fig. 2.— Left-hand axis: Precision of reference frame obtained by observing quasars, assuming *FAME* sensitivities. The three lines show how the accuracy of the frame improves when adding more quasars to some limiting magnitude R . The uppermost line corresponds to the accuracy achieved by observing the currently known quasars (Veron-Cetty & Veron 2000, VV00). The middle line shows the accuracy when one adds quasars to be identified by SDSS, 2QZ and FBQS surveys by the end of 2003, in time to be included in the input catalog. The best accuracy, lower line, is achieved if faint quasars are found all over the sky by a mission like *GALEX*. In the possible absence of *GALEX* more quasars can be found using 2MASS, the corresponding accuracy shown with circled crosses. Next to the lines and points we note the number of quasar candidates that must be put into the input catalog. Right-hand axis: Observing quasars also allows parallax systematics to be checked. This accuracy is shown normalized to 1 srad of the sky.

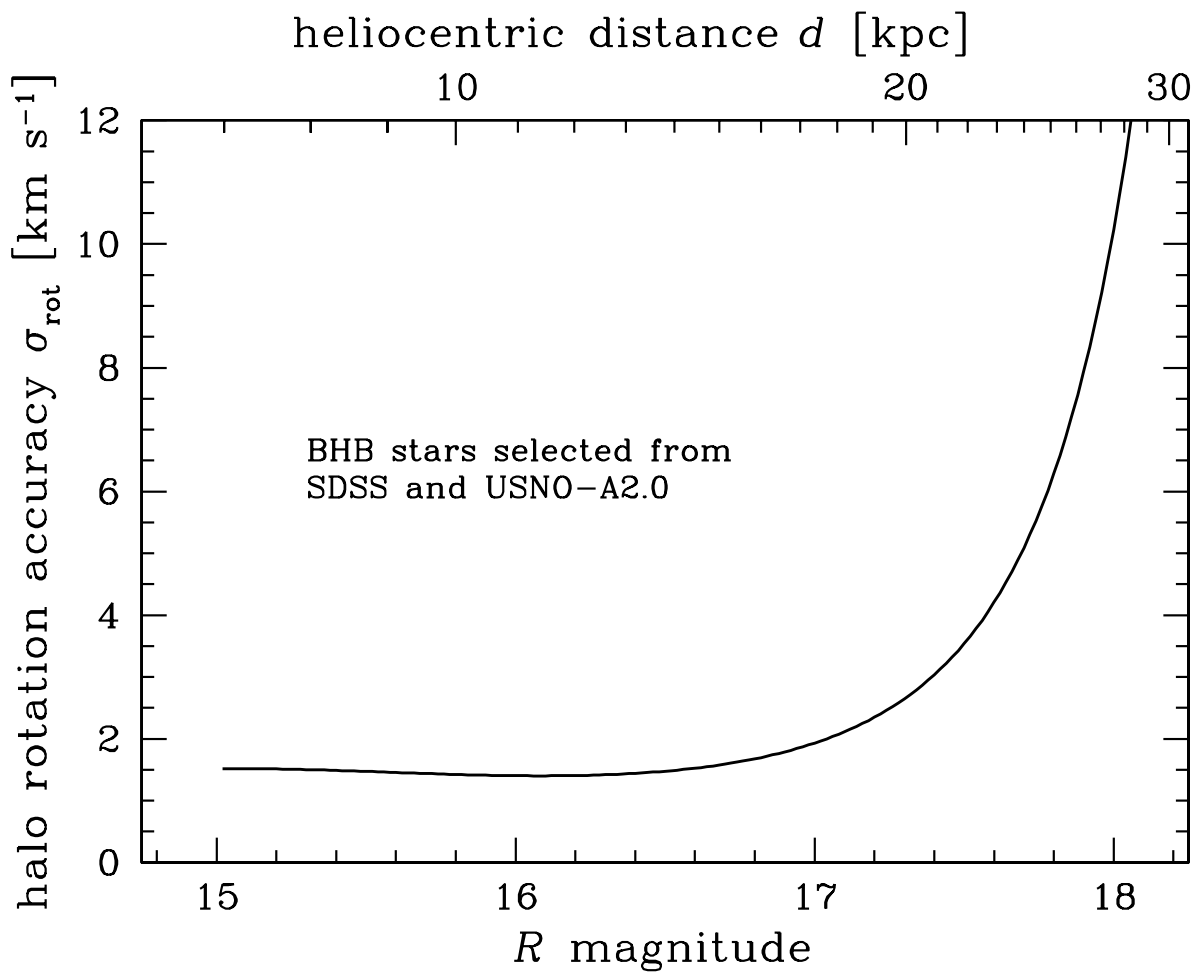


Fig. 3.— The kinematics of the halo, and especially its rotation, can be measured by selecting field blue horizontal branch stars, which have good photometric distances, and measuring their mean proper motion. We show the precision of this estimate, assuming *FAME* sensitivities, as a function of BHB stars’ R magnitude, or equivalently, their heliocentric distance. The sample is binned in 1-mag bins. Deterioration beyond $R \sim 18$ occurs mainly because the color-selected sample of A-stars becomes dominated by blue stragglers.

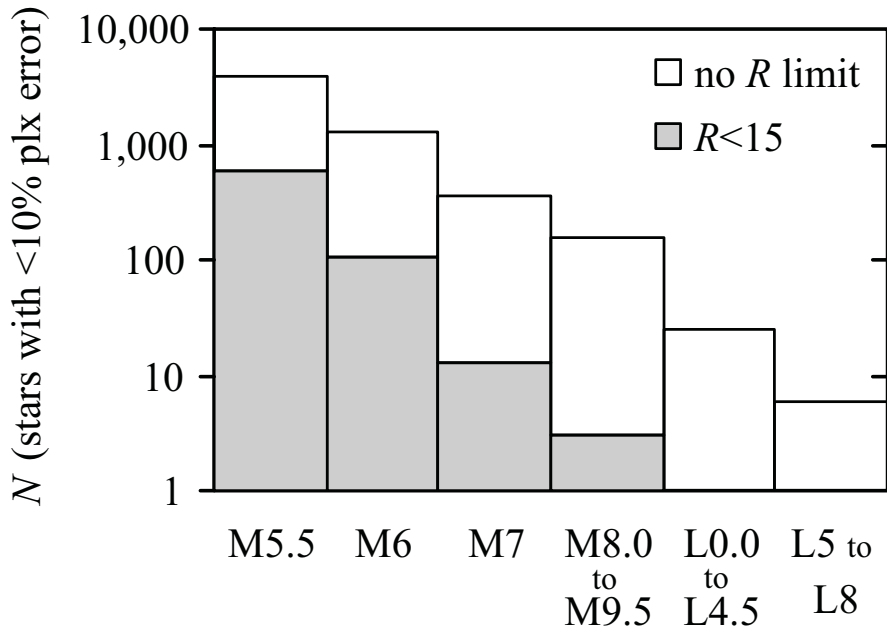


Fig. 4.— The histogram shows the number of late-type dwarfs of different spectral classes for which one can measure parallaxes with fractional error $< 10\%$, assuming *FAME* sensitivities. If objects are selected beyond the main survey magnitude limit of $R = 15$ (blank vs. grey bars), there is a significant increase in the number of good parallaxes.

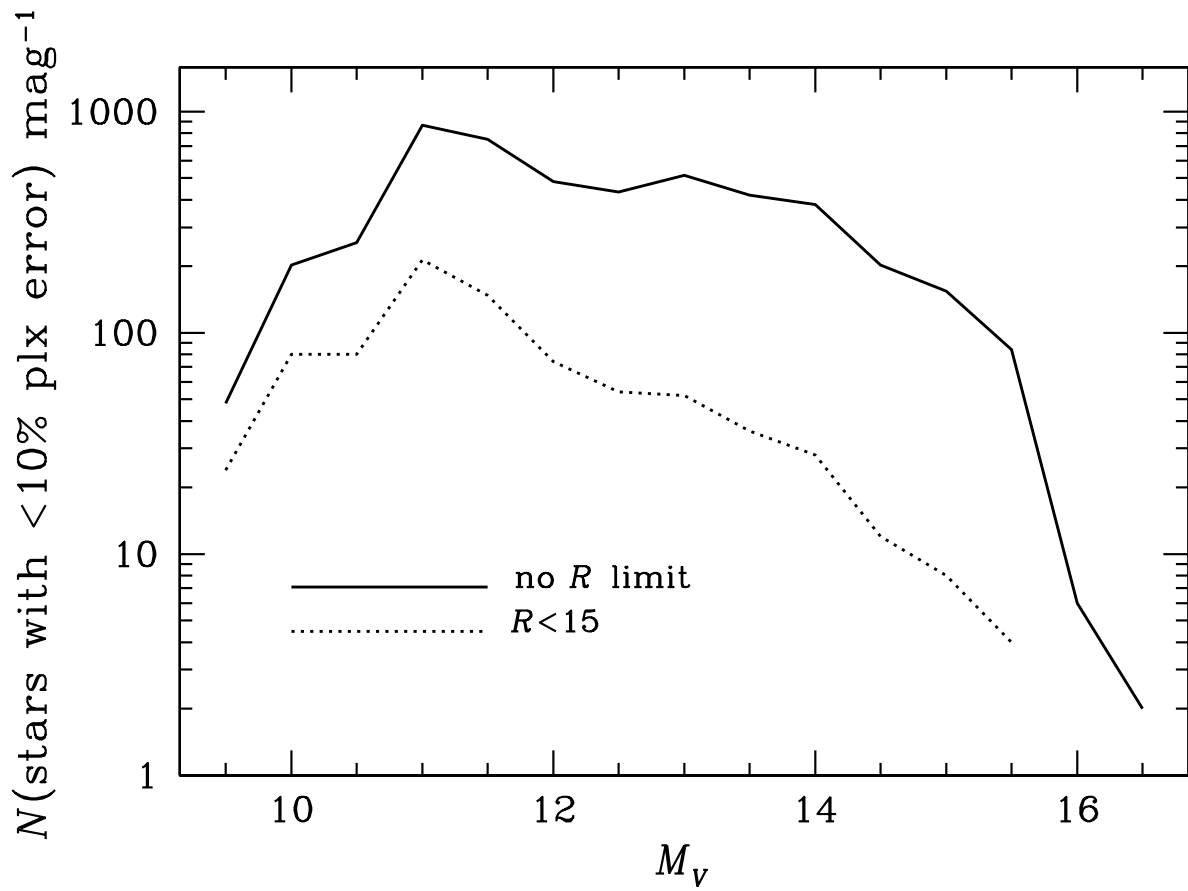


Fig. 5.— Observing WDs fainter than $R = 15$ greatly increases the number of good ($< 10\%$ fractional accuracy) parallaxes. The number (per magnitude) of good parallaxes (assuming *FAME* sensitivities) in the two cases is given as a function of WD absolute magnitude.

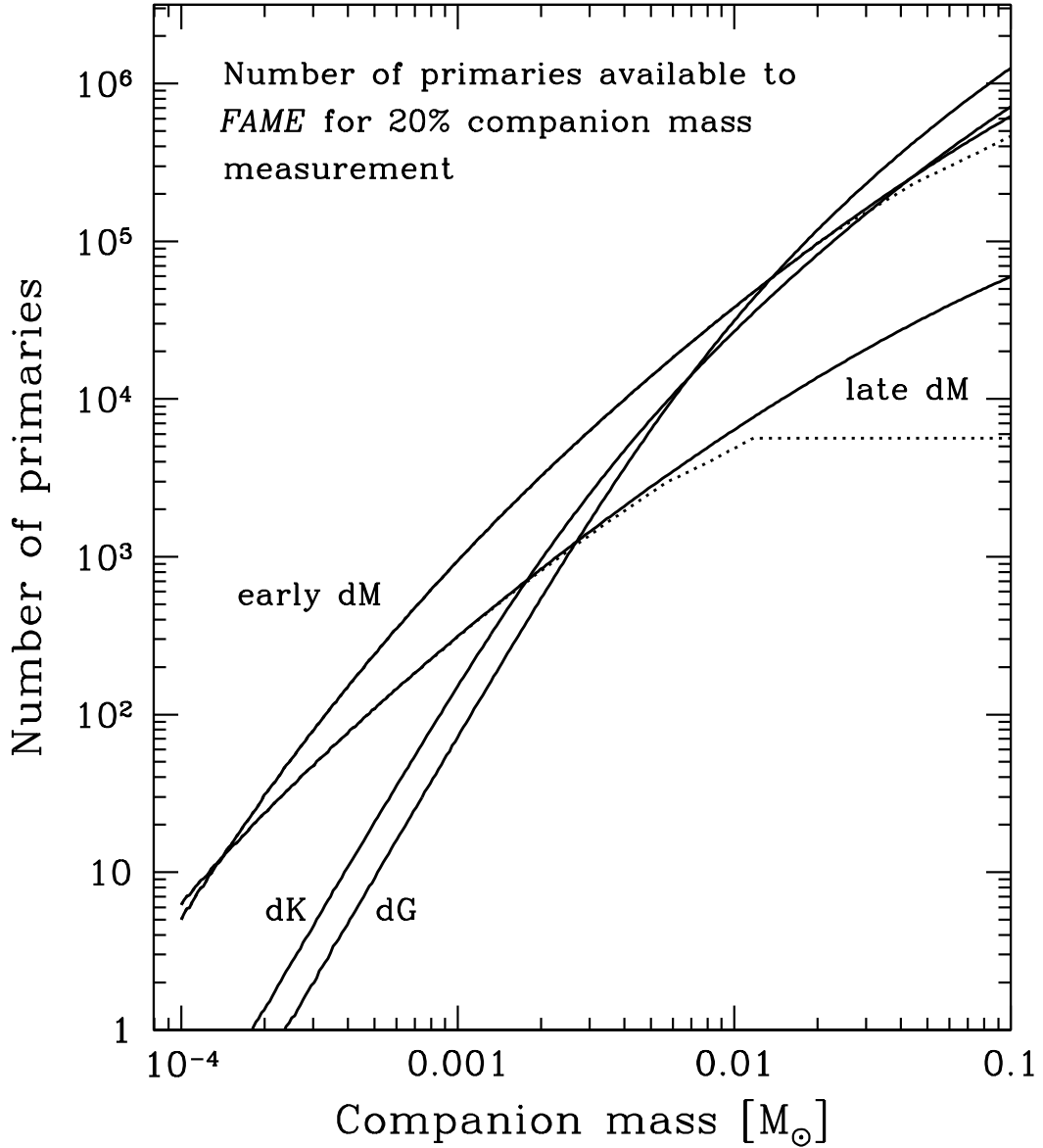


Fig. 6.— *FAME* sensitivity to planetary and brown dwarf companions. The solid curves show the number of stars for which *FAME* could detect companions in $P = 5$ yr orbits as a function of companion mass. The curves separately show G dwarfs ($3.5 < M_V < 5.5$) K dwarfs ($5.5 < M_V < 7.5$) early M dwarfs ($7.5 < M_V < 12.5$), and late M dwarfs ($12.5 < M_V < 18.5$). These curves assume that M dwarfs with $R < 18$ will be included in the input catalog. The effect of excluding stars with $R > 15$ is shown by the dashed curves. For shorter periods, P , the curves should be displaced to the right by $(2/3) \log(5 \text{ yr}/P)$.

Table 1. Rotation of the halo from BHB stars.

R mag	d kpc	N_{BHB} 10^3	N_{BS} 10^3	$\sigma(\mu_y)$ $\mu\text{as yr}^{-1}$	$\sigma(\mu_x)$ $\mu\text{as yr}^{-1}$	σ_{yy} $\mu\text{as yr}^{-1}$	σ_{xx} $\mu\text{as yr}^{-1}$	σ_{rot} km s^{-1}
15	6.9	6.3	1.1	46	66	250	502	1.52
16	11.0	8.4	2.8	27	37	98	188	1.41
17	17.4	9.0	6.7	24	28	68	107	1.94
18	27.5	7.9	11.6	79	67	239	321	10.29
19	43.7	9.3	21.6	2632	1784	6601	...	545